

# Thermal Joint Resistances of Conforming Rough Surfaces with Gas-Filled Gaps

M. Bahrami,\* M. M. Yovanovich,<sup>†</sup> and J. R. Culham<sup>‡</sup>  
*University of Waterloo, Waterloo, Ontario, Canada N2L 3G1*

**An approximate analytical model is developed for predicting the heat transfer of interstitial gases in the gap between conforming rough contacts. A simple relationship for the gap thermal resistance is derived by assuming that the contacting surfaces are of uniform temperature and that the gap heat transfer area and the apparent contact area are identical. The model covers the four regimes of gas heat conduction modes, that is, continuum, temperature jump or slip, transition, and free molecular. Effects of main input parameters on the gap and joint thermal resistances are investigated. The model is compared with other models and with more than 510 experimental data points in the open literature. Good agreement is shown over the entire range of the comparison.**

## Nomenclature

$A$	=	area, m <sup>2</sup>
$a$	=	radius of contact, m
$b_L$	=	specimens radius, m
$c_1$	=	Vickers microhardness coefficient, Pa
$c_2$	=	Vickers microhardness coefficient
$d$	=	distance between two parallel plates, m
$F$	=	external force, N
$H_{\text{mic}}$	=	microhardness, Pa
$H'$	=	$c_1(1.62\sigma'/m)^{c_2}$ , Pa
$H^*$	=	$c_1(\sigma'/m)^{c_2}$ , Pa
$Kn$	=	Knudsen number
$k$	=	thermal conductivity, W/mK
$l$	=	depth, m
$M$	=	gas parameter, m
$M_g$	=	molecular weight of gas, kg/kmol
$M_s$	=	molecular weight of solid, kg/kmol
$m$	=	mean absolute surface slope
$n_s$	=	number of microcontacts
$P$	=	pressure, Pa
$Pr$	=	Prandtl number
$Q$	=	heat flow rate, W
$q$	=	heat flux, W/m <sup>2</sup>
$R$	=	thermal resistance, K/W
$r, z$	=	cylindrical coordinates
$T$	=	temperature, K
$t$	=	dummy variable
$Y$	=	mean surface plane separation, m
$z$	=	surface height, m
$\alpha_T$	=	thermal accommodation coefficient
$\gamma$	=	ratio of gas specific heats
$\Lambda$	=	mean free path, m
$\lambda$	=	nondimensional separation $\equiv \frac{Y}{\sqrt{2}\sigma}$

$\mu$	=	ratio of molecular weights $\equiv M_g/M_s$
$\sigma$	=	rms surface roughness, m
$\sigma'$	=	$\sigma/\sigma_0$ , where $\sigma_0 = 1 \mu\text{m}$
$\phi(z)$	=	Gaussian distribution of surface heights
$\omega$	=	asperity deformation, m

## Subscripts

$a$	=	apparent
cont	=	continuum
fm	=	free molecular
$g$	=	gas, gap
$j$	=	joint
$L$	=	large
mic	=	micro
mic, e	=	effective micro
$r$	=	real
$s$	=	solid, micro
tr	=	transition
0	=	reference value
1, 2	=	solid 1, 2

## Introduction

HEAT transfer through interfaces formed by mechanical contacts has many important applications such as microelectronics cooling, nuclear engineering, and spacecraft structures design. Generally the heat transfer through the contact interfaces is associated with the presence of interstitial gases. The rate of heat transfer across the joint depends on a number of parameters: thermal properties of solids and gas, gas pressure, surface roughness characteristics, applied load, and contact microhardness.

When random rough surfaces are placed in mechanical contact, real contact occurs at the top of surface asperities called microcontacts. The microcontacts are distributed randomly in the apparent contact area  $A_a$  and located far from each other. In the real contact area  $A_r$ , the summation of microcontacts forms a small portion of the nominal contact area typically a few percent of the nominal contact area.

The geometry of a typical conforming rough contact is shown in Fig. 1, where two cylindrical bodies with a radius of  $b_L$  are placed in mechanical contact. The gap between the microcontacts is filled with an interstitial gas, and heat is transferred from one body to the other. Conduction through microcontacts and the interstitial gas in the gap between the solids are the two main paths for transferring thermal energy between contacting bodies. Thermal radiation across the gap remains small as long as the surface temperatures are not too high, that is, less than 700 K, and in most applications can be neglected.<sup>1</sup> As a result of the small real contact area and low thermal

Received 26 September 2003; revision received 23 December 2003; accepted for publication 25 December 2003; presented as Paper 2004-0821 at the AIAA 42nd Aerospace Meeting and Exhibit, Reno, NV, 5–8 January 2004. Copyright © 2004 by the authors. Published by the American Institute of Aeronautics and Astronautics, Inc., with permission. Copies of this paper may be made for personal or internal use, on condition that the copier pay the \$10.00 per-copy fee to the Copyright Clearance Center, Inc., 222 Rosewood Drive, Danvers, MA 01923; include the code 0887-8722/04 \$10.00 in correspondence with the CCC.

\*Ph.D. Candidate, Department of Mechanical Engineering, Microelectronics Heat Transfer Laboratory.

<sup>†</sup>Distinguished Professor Emeritus, Department of Mechanical Engineering, Microelectronics Heat Transfer Laboratory. Fellow AIAA.

<sup>‡</sup>Associate Professor, Director, Microelectronics Heat Transfer Laboratory.

conductivities of interstitial gases, heat flow experiences a relatively large thermal resistance passing through the joint; this phenomenon leads to a relatively high-temperature drop across the interface.

Natural convection does not occur within the fluid when the Grashof number is below 2500 (Ref. 2). (The Grashof number can be interpreted as the ratio of buoyancy to viscous forces.) In most practical situations concerning thermal contact resistance, the gap thickness between two contacting bodies is quite small ( $<0.01$  mm); thus, the Grashof number based on the gap thickness is less than 2500. Consequently, in most instances the heat transfer through the interstitial gas in the gap occurs by conduction.

In applications where the contact pressure is relatively low, the real contact area is limited to an even smaller portion of the apparent area, on the order of 1% or less. Consequently, the heat transfer takes place mainly through the interstitial gas in the gap. The relative magnitude of the gap heat transfer varies greatly with the applied load, surface roughness, gas pressure, and ratio of the thermal conductivities between the gas and solids. As the contact pressure increases, the heat transfer through the microcontacts increases and becomes more significant. Many engineering applications of thermal contact resistance (TCR) are associated with low contact pressure where air (interstitial gas) is at atmospheric pressure; therefore, modeling of the gap resistance is an important issue.

The goal of this study is to develop an approximate, comprehensive, yet simple model for determining the heat transfer through the gap between conforming rough surfaces. This model will be used in the second part of this work<sup>3</sup> to develop an analytical compact model for predicting the TCR of nonconforming rough contacts in the presence of an interstitial gas. The model covers the entire range of gas conduction heat transfer modes, that is, continuum, slip, transition, and free molecular.

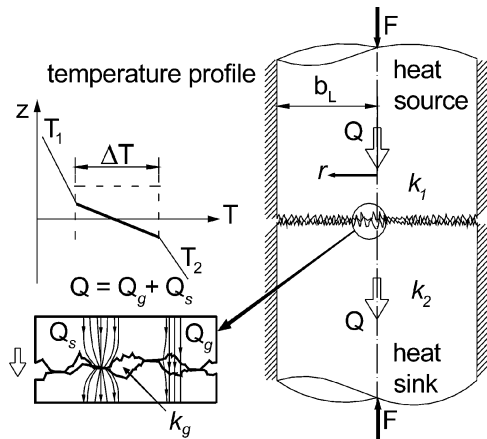


Fig. 1 Contact of conforming rough surfaces with presence of interstitial gas.

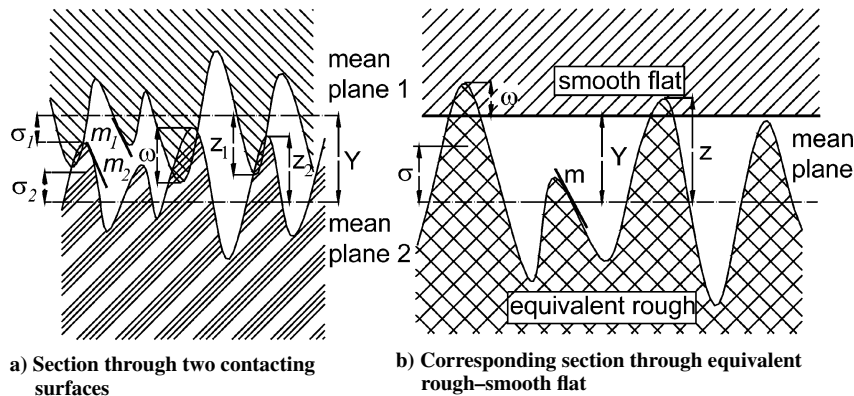


Fig. 2 Equivalent contact of conforming rough surfaces.

## Theoretical Background

TCR of conforming rough surfaces in the presence of interstitial gas includes two components, thermal constriction/spreading resistance of microcontacts,  $R_s$ , and gap thermal resistance  $R_g$ .

### Microcontacts Heat Transfer

All solid surfaces are rough, where this roughness or surface texture can be thought of as the surface heights' deviation from the nominal topography. If the asperities of a surface are isotropic and randomly distributed over the surface, the surface is called Gaussian. Williamson et al.<sup>4</sup> have shown experimentally that many of the techniques used to produce engineering surfaces give a Gaussian distribution of surface heights. Many researchers including Greenwood and Williamson<sup>5</sup> assumed that the contact between two Gaussian rough surfaces can be simplified to the contact between a single Gaussian surface, having effective surface characteristics, with a perfectly smooth surface, where the mean separation between the two contacting planes  $Y$  remains the same (Fig. 2); for more details, see Bahrami et al.<sup>6</sup> The equivalent roughness  $\sigma$  and surface slope  $m$  can be found from

$$\sigma = \sqrt{\sigma_1^2 + \sigma_2^2}, \quad m = \sqrt{m_1^2 + m_2^2} \quad (1)$$

It is common to assume that the microcontacts are isothermal.<sup>6</sup> Thermal constriction/spreading resistance of microcontacts can be modeled by using a flux tube geometry,<sup>7</sup> or if microcontacts are considered to be located far (enough) from each other, the isothermal heat source on a half-space solution<sup>8</sup> can be used. When comparison was made with the earlier mentioned solutions, that is, the flux tube and the half-space, Bahrami et al.<sup>9</sup> showed that the microcontacts can be modeled as heat sources on a half-space for engineering TCR applications.

Bahrami et al.,<sup>9</sup> assuming plastically deformed asperities and using scaling analysis techniques, developed an analytical model to predict TCR of conforming rough contacts in a vacuum,  $R_s$ ,

$$R_s = \frac{0.565 H^* (\sigma/m)}{k_s F} \quad (2)$$

where

$$k_s = 2k_1 k_2 / (k_1 + k_2), \quad H^* = c_1 (\sigma'/m)^{c_2}$$

They compared their model with more than 600 TCR experimental data points collected in a vacuum by many researchers and showed good agreement. The rms difference between Eq. (2) and the data was reported to be approximately 14%.

### Gap Heat Transfer

According to Springer,<sup>10</sup> conduction heat transfer in a gas layer between two parallel plates is commonly categorized into four heat-flow regimes: continuum, temperature jump or slip, transition, and free molecular. The parameter that characterizes the regimes is the

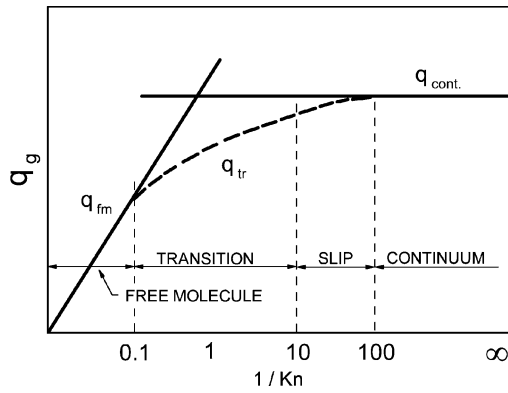


Fig. 3 Heat flux regimes as function of Knudsen number.

Knudsen number

$$Kn = \Lambda/d \quad (3)$$

where  $\Lambda$  and  $d$  are the molecular mean free path and the distance separating the two plates, respectively. The molecular mean free path is defined as the average distance a gas molecule travels before it collides with another gas molecule, and it is proportional to the gas temperature and inversely proportional to the gas pressure,<sup>11</sup>

$$\Lambda = (P_0/P_g)(T_g/T_0)\Lambda_0 \quad (4)$$

where  $\Lambda_0$  is the mean free path value at some reference gas temperature  $T_0$  and pressure  $P_0$ .

Figure 3 shows the four heat flow regimes, that is, continuum, temperature jump or slip, transition, and free molecular, as a function of inverse Knudsen number. In the continuum regime, where  $Kn \ll 1$ , the heat transfer between the plates takes place mainly through collisions of the gas molecules, and the rate of heat transfer is independent of the gas pressure but varies with the gas temperature. Fourier's law of conduction can be used in this regime. As the gas pressure is reduced, the intermolecular collisions become less frequent and the heat exchange of energy between gas molecules and the plates starts to affect the heat transfer between the plates. According to Kennard,<sup>11</sup> for  $0.01 \leq Kn \leq 0.1$ , the heat exchange exhibits a temperature-jump behavior. The energy transfer between the gas molecules and the plate is incomplete, and a discontinuity of temperature develops at the wall-gas interface. At the extreme end of very low gas pressure (or high gas temperature), the free-molecular regime,  $Kn \geq 10$ , intermolecular collision is rare, and the essential mechanism for heat transfer in this regime is the energy exchange between the gas molecules and the plates. The region between the temperature-jump and the free-molecular regimes, that is,  $0.1 \leq Kn \leq 10$ , is called the transition region in which intermolecular collisions and the energy exchange between the gas molecules and the plate walls are both important.

Using Maxwell's theory for temperature-jump distance, Kennard<sup>11</sup> modeled the gas conduction between two parallel plates for temperature jump as  $q_g = k_g(T_1 - T_2)/(d + M)$ . Yovanovich<sup>12</sup> proposed that Kennard's expression can be used to predict the gas conduction for all four regimes. It can be seen that for the continuum regime  $M \rightarrow 0$ ; thus,  $M \ll d$ , for the free molecular regime  $M \rightarrow \infty$  and  $M \gg d$  also. Therefore, heat flux for all four flow regimes can be effectively represented by

$$q_g = [k_g/(d + M)](T_1 - T_2) \quad (5)$$

where  $T_1$ ,  $T_2$ ,  $k_g$ , and  $q_g$  are the uniform temperatures of the two parallel plates, gas thermal conductivity, and the gap heat flux, respectively. When Eq. (5) and the definition of thermal resistance, that is,  $R = \Delta T/Q$ , are used, gap thermal resistance can be found from

$$R_g = (d + M)/(k_g A_g) \quad (6)$$

where  $A_g = A_a - A_r$  is the gap heat transfer area. The gas parameter  $M$  is defined as

$$M = [(2 - \alpha_{T1})/\alpha_{T1} + (2 - \alpha_{T2})/\alpha_{T2}][2\gamma/(1 + \gamma)](1/Pr)\Lambda \quad (7)$$

where  $\alpha_{T1}$ ,  $\alpha_{T2}$ , and  $\Lambda$  are thermal accommodation coefficients corresponding to the gas-solid combination of plates 1 and 2 and the molecular mean free path at  $P_g$  and  $T_g$ , respectively.

Thermal accommodation coefficient  $\alpha_T$  depends on the type of the gas-solid combination and is in general very sensitive to the condition of the solid surfaces. It represents the degree to which the kinetic energy of a gas molecule is exchanged while in collision with the solid wall. Song and Yovanovich<sup>13</sup> purposed a correlation for predicting  $\alpha_T$  for engineering surfaces,

$$\alpha_T = \exp\left[-0.57\left(\frac{T_s - T_0}{T_0}\right)\right] \left(\frac{M_g^*}{6.8 + M_g^*}\right) + \frac{2.4\mu}{(1 + \mu)^2} \left\{1 - \exp\left[-0.57\left(\frac{T_s - T_0}{T_0}\right)\right]\right\} \quad (8)$$

where for monatomic gases

$$M_g^* = M_g$$

and for diatomic/polyatomic gases

$$M_g^* = 1.4M_g$$

where  $T_0 = 273$  K. Equation (8) is general and can be used for any combination of gases and solid surfaces for a wide temperature range. The agreement between the predicted values and the experimental data is within 25%.

Yovanovich et al.<sup>14</sup> developed a statistical sophisticated model (here called the integral model) to predict thermal gap conductance between conforming rough surfaces. The integral model takes into consideration the variation in the local gap thickness due to the surface roughness. It assumes that the temperature of the two surfaces in contact are uniform and the interface gap consists of many elemental flux tubes of different thermal resistances. The resistances of these elemental flux tubes are then assumed to be in parallel, which results in an overall gap conductance in an integral form that may be represented in thermal resistance form as

$$R_g = \sqrt{2\pi}Y \int \left\{ A_g k_g \int_0^\infty \frac{\exp[-(Y/\sigma - t/\sigma)^2/2]}{(t/\sigma)/(Y/\sigma) + M/Y} d\left(\frac{t}{\sigma}\right) \right\} \quad (9)$$

where  $R_g$ ,  $t$ ,  $k_g$ ,  $A_g$ , and  $Y$  are thermal gap resistance, length of the elemental flux tube or the local gap thickness, thermal conductivity of the gas, gap heat transfer area, and mean plane separation distance, respectively.

Equation (9) is in integral form, and its evaluation requires a numerical integration. Song<sup>15</sup> correlated Eq. (9) and proposed an expression that can be written as follows:

$$R_g = \frac{Y}{k_g A_g} \left[ 1 + \frac{M}{Y} + \frac{0.304(\sigma/Y)}{(1 + M/Y)} - \frac{2.29(\sigma/Y)^2}{(1 + M/Y)^2} \right] \quad (10)$$

### Present Model

Implementing Eq. (9) results in a complicated integral for the effective thermal resistance of the microgaps in the second part of this study,<sup>3</sup> that is, nonconforming rough joints in a gaseous environment. To avoid a numerical solution, an approximate analytical model is developed for predicting the heat transfer of interstitial gases in the gap between conforming rough joints.

The geometry of the contact is shown in Figs. 1 and 4, where the contact of two rough surfaces is simplified to the contact of an equivalent rough and a smooth plate. It is assumed that the contacting surfaces are Gaussian and the asperities deform plastically. Heat transferred through the joint includes the microcontacts  $Q_c$  and the gas  $Q_g$  heat flows.

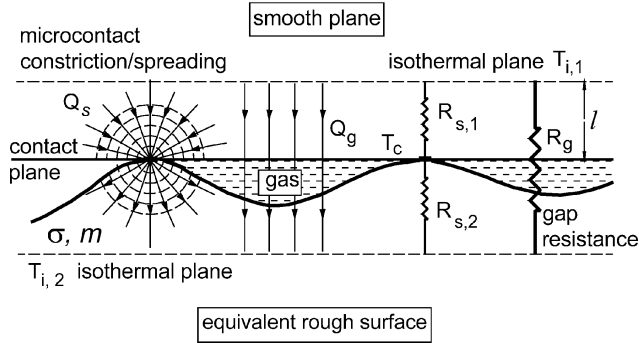


Fig. 4 Microcontacts and gap heat flows, conforming rough joints.

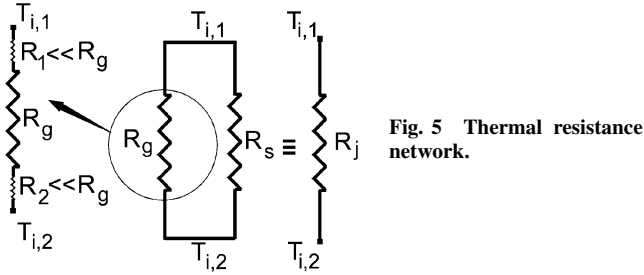


Fig. 5 Thermal resistance network.

As already mentioned, microcontacts can be modeled as isothermal heat sources on a half-space. Considering circular shape microcontacts with the radius  $a_s$  on the order of micrometers, isothermal planes with some temperatures  $T_{i,1}$  and  $T_{i,2}$  at depth  $l$  must exist in bodies one and two, respectively (Fig. 4). Under vacuum conditions, that is,  $Q_g = 0$ , the distance between the isothermal planes and the contact plane is  $l = 40a_s \sim 40 \mu\text{m}$  (Ref. 1). When the gas pressures is increased, heat flow through the joint increases and distance  $l$  decreases. Because microcontacts are assumed to be flat and located in the contact plane, isothermal planes  $T_{i,1}$  and  $T_{i,2}$  are parallel to the contact plane. Therefore, TCR can be represented by two sets of thermal resistances in parallel between isothermal planes  $T_{i,1}$  and  $T_{i,2}$ ,

$$R_j = (1/R_s + 1/R_g)^{-1} \quad (11)$$

where

$$R_s = \left( \sum_{i=1}^{n_s} \frac{1}{R_{s,i}} \right)^{-1}$$

and  $n_s$  are the equivalent thermal resistance of the microcontacts and the number of microcontacts, respectively. The thermal resistance of the microcontacts  $R_s$  is determined using Eq. (2).

Figure 5 shows the thermal resistance network of the joint. Because the thermal resistances are considered to be in parallel between two isothermal plates  $T_{i,1}$  and  $T_{i,2}$ , the gap resistance  $R_g$  has three components, the gap resistance and  $R_1$  and  $R_2$ , which correspond to the bulk thermal resistance of the solid layers in bodies 1 and 2, respectively. The bulk resistances  $R_1$  and  $R_2$  can be considered negligible in relation to  $R_g$  because the gas thermal conductivity is much lower than the conductivity of the solids, that is,  $k_g/k_s \leq 0.01$ .

$$R_{g,\text{total}} = \underbrace{R_1 + R_2}_{\ll R_g} + (d + M)/(k_g A_g) = R_g \quad (12)$$

where  $R_1 = l/k_{s,1} A_g$ ,  $R_2 = l/k_{s,2} A_g$ , and  $A_g = A_a - A_r$  is the gas heat transfer area.

The real contact area is a very small portion of the apparent contact area, that is,  $A_r \ll A_a$ ; thus, it can be assumed that  $A_g = A_a$ . As a result, the heat transferred through the microgaps between rough surfaces can be replaced by the gas heat transfer between two isothermal parallel plates that are located at an effective distance  $d$  from each other. In addition, the gap heat transfer area becomes

the apparent contact area  $A_a$ . As already mentioned, Eq. (5) can be used to determine the heat transfer between two isothermal surfaces through an interstitial gas for all four flow regimes.

To determine the gap thermal resistance, the effective distance between contacting bodies,  $d$ , is required. For contact of Gaussian rough surfaces with the mean separation  $Y$ , the statistical effective plane separation over the contact area,  $d$ , can be found from

$$d = \int_{-\infty}^Y (Y - z)\phi(z) dz \quad (13)$$

where  $\phi(z)$  is the Gaussian distribution defined as

$$\phi(z) = (1/\sqrt{2\pi}\sigma) \exp(-z^2/2\sigma^2) \quad (14)$$

where  $z$  and  $\sigma$  are surface heights and the equivalent rms surface roughness, respectively. When Eq. (14) is substituted into Eq. (13), after evaluating and simplifying,  $d$  becomes

$$d = (\sigma/\sqrt{2\pi}) [\sqrt{\pi}(1 + \text{erf } \lambda)\lambda + \exp(-\lambda^2)] \quad (15)$$

where  $\lambda = Y/\sqrt{2}\sigma$  is the nondimensional mean separation. Equation (15) is plotted over a wide range of  $\lambda$ , that is,  $1 \leq \lambda \leq 5$  in Fig. 6; a nearly linear behavior can be observed over the comparison range. Thus, a linear relationship for  $d$  can be derived in the form

$$d = \sqrt{2}\sigma\lambda = Y \quad (16)$$

The maximum relative difference between Eqs. (15) and (16) is less than 1.7% over the entire range of  $\lambda$ . Equation (16) indicates that  $d$  is identical to the mean separation between two planes.

For conforming rough contacts assuming plastic deformation of asperities, it can be shown<sup>7</sup>

$$P/H_{\text{mic}} = \frac{1}{2} \text{erfc } \lambda \quad (17)$$

or

$$\lambda = \text{erfc}^{-1}(2P/H_{\text{mic}}) \quad (18)$$

where  $H_{\text{mic}}$ ,  $P = F/A_a$ , and  $\text{erfc}^{-1}(\cdot)$  are the effective microhardness of the softer material in contact, contact pressure, and inverse complementary error function, respectively.

Microhardness depends on several parameters: mean surface roughness  $\sigma$ , mean absolute slope of asperities,  $m$ , type of material, method of surface preparation, and applied pressure. Hegazy<sup>16</sup> proposed correlations in the form of the Vickers microhardness for calculating surface microhardness. Song and Yovanovich<sup>17</sup> developed an explicit expression relating microhardness to the applied pressure,

$$P/H_{\text{mic}} = (P/H')^{1/(1+0.071c_2)} \quad (19)$$

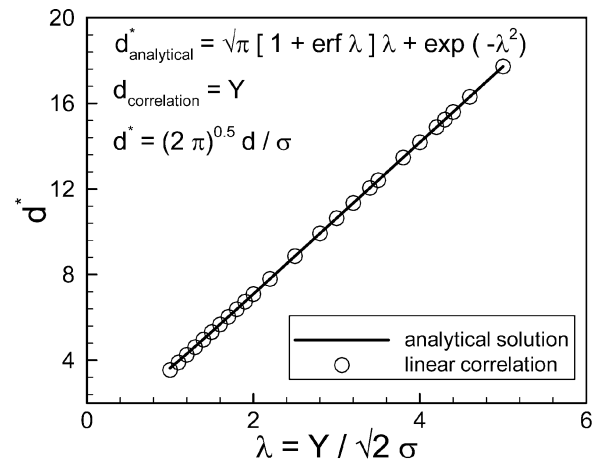


Fig. 6 Comparison between analytical solution and linear correlation of plane separation  $d$ .

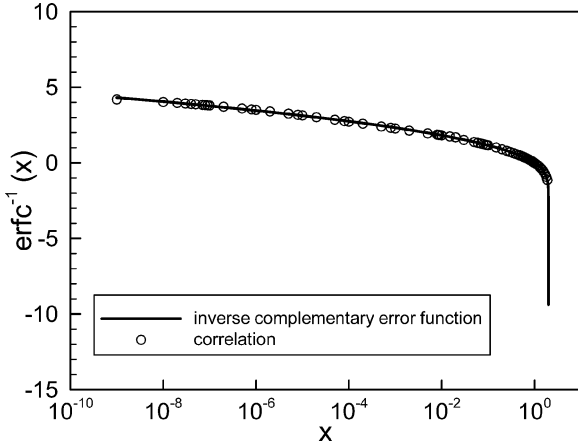


Fig. 7 Inverse complementary error function.

where  $H' = c_1(1.62\sigma'/m)^{c_2}$ ,  $\sigma' = \sigma/\sigma_0$ , and  $\sigma_0 = 1 \mu\text{m}$ . In situations where an effective value for microhardness  $H_{\text{mic},e}$  is known, the microhardness coefficients can be replaced by  $c_1 = H_{\text{mic},e}$  and  $c_2 = 0$ . When Eq. (19) is substituted in Eq. (18),

$$\lambda = Y/\sqrt{2\sigma} = \text{erfc}^{-1}(2P/H') \quad (20)$$

where for convenience parameter  $1/(1+0.071c_2)$  is assumed to be 1. Note that  $-0.35 \leq c_2 \leq 0$ .

Yovanovich<sup>12</sup> proposed an accurate correlation for determining the inverse complementary error function,  $\text{erfc}^{-1}(x) = 0.837[-\ln(1.566x)]^{0.547}$  for  $x \leq 0.01$ , with the maximum relative error less than 0.25%. Because a broader range of  $\text{erfc}^{-1}(\cdot)$  is needed in this study (especially the second part), with use of Maple,<sup>18</sup> a set of expressions for determining  $\text{erfc}^{-1}(x)$  are developed that cover a range of  $10^{-9} \leq x \leq 1.9$ ,

$$\text{erfc}^{-1}(x) = \begin{cases} \frac{1}{0.218 + 0.735x^{0.173}} & 10^{-9} \leq x \leq 0.02 \\ \frac{1.05(0.175)^x}{x^{0.12}} & 0.02 < x \leq 0.5 \\ \frac{1-x}{0.707 + 0.862x - 0.431x^2} & 0.5 < x \leq 1.9 \end{cases} \quad (21)$$

The maximum relative difference between Eq. (21) and  $\text{erfc}^{-1}(x)$  is less than 2.8% for the range  $10^{-9} \leq x \leq 1.9$ . Figure 7 shows the comparison between  $\text{erfc}^{-1}(x)$  and Eq. (21).

When Eqs. (16) and (20) are combined, the gas thermal resistance can be found from

$$R_g = (1/k_g A_a) \left[ M + \frac{\sqrt{2\sigma} \text{erfc}^{-1}(2P/H')}{Y} \right] \quad (22)$$

The thermal joint resistance can be calculated combining Eqs. (11), (2), and (22).

#### Comparison Between Present and Integral Models

To compare the present model Eq. (22) with the integral model Eq. (10), both expressions are nondimensionalized and rewritten in the following form:

$$\frac{k_g A_a R_g}{Y} = \begin{cases} 1 + \frac{M}{Y} & \text{present model} \\ 1 + \frac{M}{Y} + \frac{0.304(\sigma/Y)}{(1+M/Y)} - \frac{2.29(\sigma/Y)^2}{(1+M/Y)^2} & \text{integral model} \end{cases} \quad (23)$$

Table 1 Relative percent difference between present and integral gap models

$M/Y$	$Y/\sigma$		
	3.50	3.00	2.50
0.001	9.97	15.26	24.39
0.01	9.63	14.76	23.64
0.10	6.87	10.74	17.48
0.50	1.68	3.04	5.45
1.00	0.17	0.65	1.54
2.00	-0.27	-0.18	0.01
10	-0.06	-0.06	-0.07
20	-0.02	-0.02	-0.02
50	0.00	0.00	0.00
100	0.00	0.00	0.00
$6 \times 10^6$	0.00	0.00	0.00

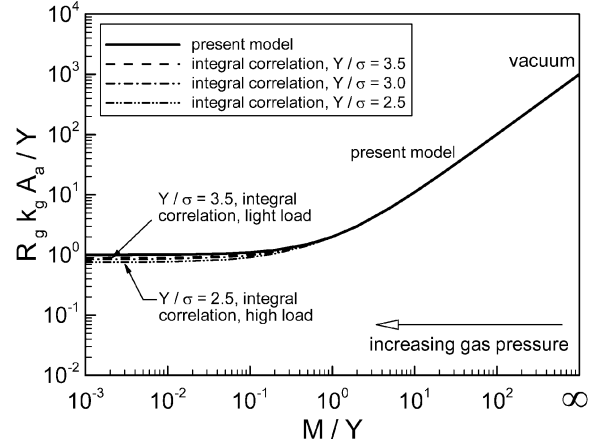


Fig. 8 Comparison of present model and Song<sup>15</sup> correlation.

The ratio  $Y/\sigma$  appears in the integral model correlation, which can be interpreted as the level of loading. For a fixed contact geometry, as the applied load increases,  $Y$  decreases and this parameter becomes smaller. Three values of  $Y/\sigma$  in Eq. (23) are included in the comparison, 2.5, 3, and 3.5, which represent three levels of loading from high to low, respectively (Fig. 8). The other parameter,  $M/Y$ , is varied over a wide range,  $10^{-3} < M/Y \leq \infty$ , from vacuum to atmospheric pressure conditions, respectively. Table 1 lists relative differences between the present and the integral gap models. As shown, the relative differences are negligible where  $M/Y \geq 1$ , that is, slip to free-molecular regimes. As the parameter  $M/Y$  becomes smaller, that is, continuum regime (atmospheric gas pressure condition), the relative difference becomes larger. It can also be seen that the relative difference is larger at smaller values of  $Y/\sigma$ , that is, higher loads. As already mentioned, the total or joint resistance is the parallel combination of the microcontacts  $R_s$  and the microgaps  $R_g$  resistances. Note that the contribution of the gas heat transfer is relatively smaller in higher loads because the microcontact resistance is smaller and controls the joint resistance. As a result, the relative difference in the joint resistances determined from the present and the integral gap models becomes smaller.

#### Parametric Study

The thermal joint resistance  $R_j$  can be nondimensionalized with respect to the thermal resistance of the microcontacts  $R_s$

$$R_j^* = R_j/R_s = 1/(1 + R_s/R_g) \quad (24)$$

Equation (24) is plotted in Fig. 9; in the limit where  $R_g$  approaches infinity (vacuum condition), as expected  $R_j^*$  approaches 1 or  $R_j = R_s$ . As  $R_s/R_g$  increases,  $R_j^*$  asymptotically approaches  $R_g^*$ . The ratio of  $R_s/R_g$  decreases either by a decrease in the gas pressure or an increase in the external load.

Effects of external load (applied pressure) and gas pressure on thermal gap and joint resistances are investigated and shown in

**Table 2** Input parameters for a typical SS-nitrogen joint

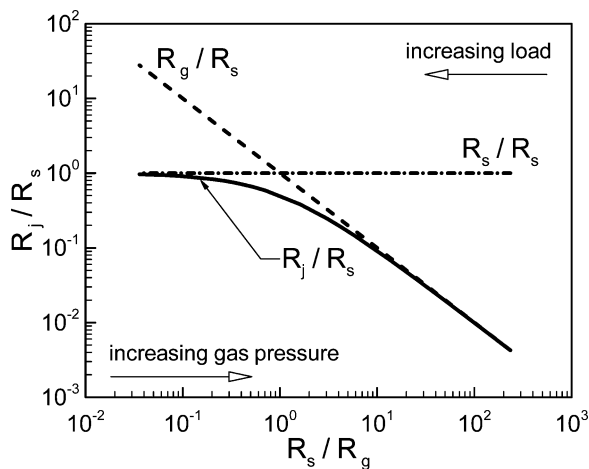
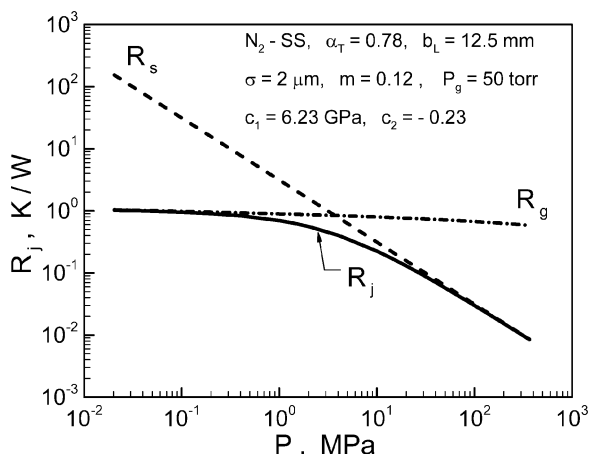
Parameter	Value
$\alpha_T$ (SS - N <sub>2</sub> )	0.78
$b_L$	12.5 mm
$\sigma$	2 $\mu$ m
$m$	0.12
$F$	35 N
$\Lambda_0$	62.8 nm
$k_g, k_s$	0.031, 20 W/mK
$c_1, c_2$	6.23 GPa, -0.23

**Table 3** Range of parameters for experimental data

Parameter	Range
$F$	69.7–4357 N
$P$	0.14–8.8 MPa
$k_s$	19.2–72.5 W/mK
$m$	0.08–0.205
$P_g$	10 <sup>-5</sup> –760 torr
$\alpha_T$	0.55–0.9
$\sigma$	1.52–11.8 $\mu$ m

**Table 4** Properties of gases

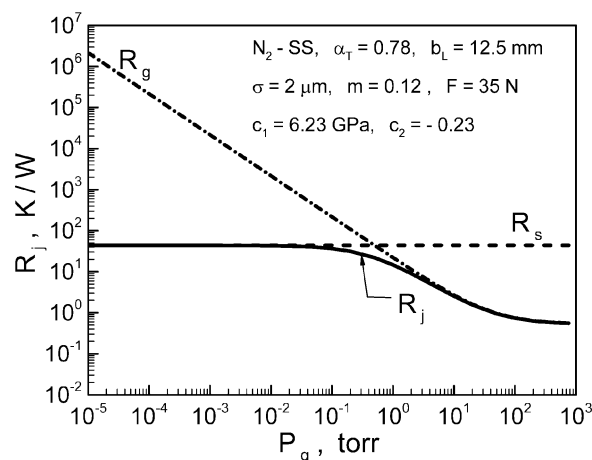
Gas	$k_g$ , W/mK	Pr	$\alpha_T$	$\gamma$	$\Lambda_0$ , nm
Ar	0.018 + 4.05 $\times 10^{-5}T$	0.67	0.90	1.67	66.6
He	0.147 + 3.24 $\times 10^{-4}T$	0.67	0.55	1.67	186.0
N <sub>2</sub>	0.028 + 5.84 $\times 10^{-5}T$	0.69	0.78	1.41	62.8

**Fig. 9** Nondimensional thermal joint resistance.**Fig. 10** Effect of load on thermal joint resistance.

Figs. 10 and 11, respectively. Input parameters of a typical contact are shown in Table 2; contacting surfaces are stainless steel and the interstitial gas is nitrogen at 373.15 K and 50 torr.

The external load is varied over a wide range,  $10 \leq F \leq 180,000$  N, to study the effect of load on thermal joint resistance. As shown in Fig. 10, at light loads the gap thermal resistance is the controlling component of thermal joint resistance. Thus, most of the heat transfer occurs through the gas. As the load increases,  $R_s$ , which is inversely proportional to the load [Eq. (2)], decreases. As a result, the mean separation between the two bodies,  $Y$ , decreases, which leads to a decrease in  $R_g$ . In higher loads,  $R_s$  is smaller and controls the joint resistance.

To study the effect of gas pressure on the thermal joint resistance, the gas pressure is varied over the range of  $10^{-5} \leq P_g \leq 760$  torr, while all other parameters in Table 2 are held constant. As shown in Fig. 11, at very low gas pressures (vacuum)  $R_g$  is large. Thus  $R_s$  controls the joint resistance by increasing the gas pressure, thermal gas resistance decreases, and  $R_g$  becomes the controlling component.

**Fig. 11** Effect of nitrogen pressure on thermal joint resistance.

### Comparison with Experimental Data

The present model is compared with more than 510 experimental data points collected by Hegazy<sup>16</sup> and Song.<sup>15</sup> The geometry of the experimental set up is shown in Fig. 1. Tests include two flat rough cylindrical specimens with the same radius  $b_L = 12.5$  mm, which are placed in contact by applying an external load in a chamber filled with an interstitial gas. To minimize the radiation and convection heat transfer to the surroundings, the lateral surfaces of the specimens were insulated. Test specimens were made of stainless steel (SS) 304 and nickel 200, and interstitial gases were argon, helium, and nitrogen. The gas pressure was varied from atmospheric pressure 760 to vacuum  $10^{-5}$  torr. As summarized in Table 3, the experimental data cover a relatively wide range of mechanical, thermal, and surface characteristics.

Thermal properties of argon, helium, and nitrogen are listed in Table 4.<sup>15,16</sup> Note that the reference mean free paths,  $\Lambda_0$  nm, are at 288 K and 760 torr and temperature in  $k_g$  correlations must be in degrees Celsius.

### Hegazy<sup>16</sup> Experimental Data

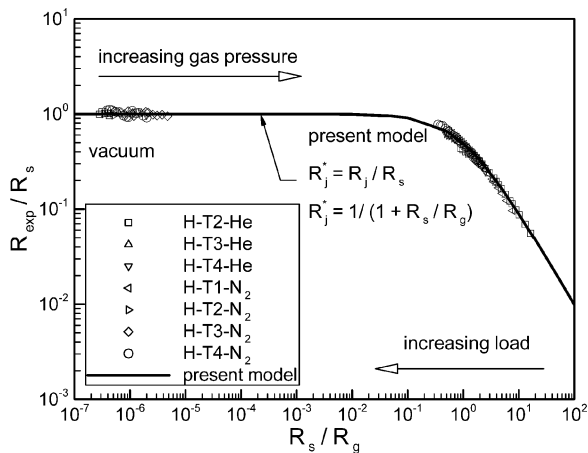
Hegazy<sup>16</sup> collected more than 160 data points during four sets of experiments performed on SS 304 joints tested in nitrogen and helium. Low thermal conductivity and high microhardness values of SS 304 provide a reasonable set of extremes for verification of the gap model. Table 5 lists the experiment numbers, solid-gas combinations, gas pressure, surface roughness, and slope of the Hegazy experimental data. The nominal contact pressure was varied from 0.459 to 8.769 MPa throughout the tests. The average gas temperature and thermal conductivity of SS 304 were reported in the range of 170–220°C and 20.2 W/mK, respectively.

**Table 5 Summary of Hegazy experiments<sup>16</sup>**

Test	Gas	$P_g$ , torr	$\sigma$ , $\mu\text{m}$	$m$
T1	N <sub>2</sub>	562–574	5.65	0.153
T2	N <sub>2</sub> , He	Vacuum, 40	5.61	0.151
T3	N <sub>2</sub> , He	Vacuum, 40	6.29	0.195
T4	N <sub>2</sub> , He	Vacuum, 40	4.02	0.168

**Table 6 Summary of Song experiments<sup>15</sup>**

Test	Solid–gas	$P$ , MPa	$\sigma$ , $\mu\text{m}$	$m$
T1	SS–N <sub>2</sub> , Ar, He	0.595–0.615	1.53	0.090
T2	SS–N <sub>2</sub> , Ar, He	0.467–0.491	4.83	0.128
T3	Ni–N <sub>2</sub> , Ar, He	0.511–0.530	2.32	0.126
T4	Ni–N <sub>2</sub> , Ar, He	0.371–0.389	11.8	0.206
T5	SS–N <sub>2</sub> , He	0.403–7.739	6.45	0.132
T6	SS–N <sub>2</sub> , He	0.526–8.713	2.09	0.904
T7	Ni–N <sub>2</sub> , He	0.367–6.550	11.8	0.206

**Fig. 12 Comparison of present model with Hegazy data.<sup>16</sup>**

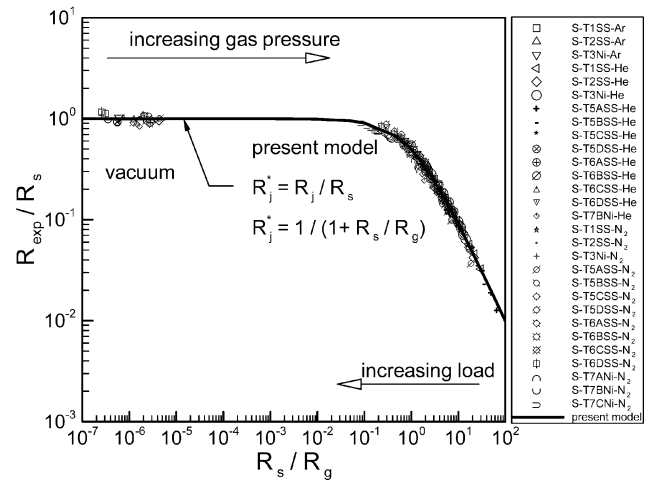
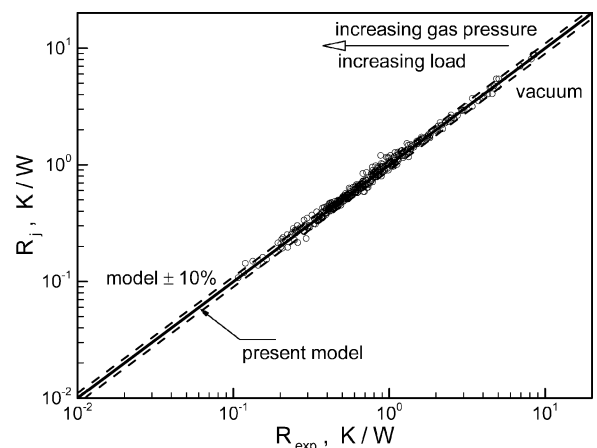
The experimental data are nondimensionalized and compared with the present model in Fig. 12. The maximum uncertainty of the experimental data was reported to be 5.7%. As can be seen in Fig. 12, the present model shows good agreement, where the rms difference between the model and the data is approximately 6%.

#### Song<sup>15</sup> Experimental Data

Song<sup>15</sup> conducted seven sets of experiments performed on nickel 200 and SS 304 joints tested in argon, helium, and nitrogen. In addition to SS 304 specimens, nickel 200 was chosen, which has a thermal conductivity of about 3.5 times that of SS 304 (at 170°C). Thus, the contribution of the microcontacts to the joint heat transfer is significantly greater than that of a SS 304 joint of similar conditions. Table 6 summarizes the experiment numbers, solid–gas combinations, range of the nominal contact pressure, and surface roughness and slope of the Song's experimental data. The tests were conducted in the following order: 1) at least one vacuum test, 2) series of helium tests at various gas pressures, 3) vacuum test, 4) series of nitrogen tests at various gas pressures, 5) vacuum test, and 6) series of argon tests at various gas pressures. The gas pressure was varied from 10<sup>-5</sup> to approximately 650 torr. The mean contact temperature, that is, the mean gas temperature was maintained at approximately 170°C, and the average thermal conductivities of SS 304 and Ni 200 were reported as 19.5 and 71.2 W/mK, respectively.

Experiments T5–T7 involved gas tests at several load levels, indicated by letters A, B, C, and D in Fig. 13. The purpose of these tests was to observe the load dependence of the thermal gap resistance. As can be seen in Table 6, only helium and nitrogen were used in these tests because it had been concluded from tests T1–T4 that argon behaves essentially the same as nitrogen.

Approximately 350 data points are nondimensionalized and compared with the present model in Fig. 13. The maximum uncertainty

**Fig. 13 Comparison of present model with Song data.<sup>15</sup>****Fig. 14 Comparison of present model with data of Song<sup>15</sup> and Hegazy.<sup>16</sup>**

of the experimental data was reported to be less than 10%. As shown in Fig. 13, the present model shows good agreement with the data over the entire range of the comparison. The rms difference between the model and the data is 8.1 percent.

Figure 14 shows the comparison between the present model and both Hegazy and Song experimental data. The rms difference between the present model and experimental is approximately 7.3 percent.

## Conclusions

Heat transfer of an interstitial gas between conforming random rough joints was studied. When the general expression for heat transfer between two isothermal parallel plates proposed by Yovanovich<sup>12</sup> was used, an approximate analytical model was developed. The model covers the four regimes of heat conduction modes of gas, that is, continuum, temperature jump or slip, transition, and free molecular and accounts for gas and solid mechanical and thermal properties, gas pressure and temperature, surface roughness, and applied load.

It was shown that the gas and the microcontacts thermal resistances are in parallel. With use of a statistical relation for Gaussian rough surfaces, it was illustrated that for engineering applications the effective separation over the contact area,  $d$ , is identical to the mean separation between two contacting surfaces  $Y$ . With the knowledge that the real contact area is a very small portion of the apparent area, it was assumed that the gap heat transfer area is identical to the apparent area. Also uniform temperatures for the contacting surfaces were assumed. These assumptions simplified the analysis, and a simple relationship for the gap thermal resistance was derived. A

correlation for inverse complementary error function was developed that determines  $\text{erfc}^{-1}(\cdot)$  within 2.8% relative error.

The influence of the main input parameters on the gap and joint thermal resistances revealed the following:

1) With constant gas pressure, at light loads  $R_g$  was the controlling part of  $R_j$ . Thus most of the heat transfer occurred through the gas. By the increase of the external load  $R_j$ ,  $R_s$  and  $R_g$  decreased and  $R_s$  became relatively small and controlled the joint resistance.

2) With constant load, at very low gas pressures (vacuum)  $R_g$  was large. Thus  $R_s$  controlled the joint resistance, by the increase of the gas pressure,  $R_g$  decreased and became the controlling component of  $R_j$ .

The present model was compared with the integral model (Yovanovich et al.<sup>14</sup>). It was shown that the relative differences between the present and the integral model were negligible for the slip to free-molecular regimes. The relative difference became larger for the continuum regime (atmospheric gas pressure condition) at relatively high loads. When it is considered that the contribution of the gas heat transfer is relatively small at higher loads, the relative difference in the total joint resistances determined from the present and the integral gap model became smaller.

The present model was compared with more than 510 experimental data points collected by Hegazy<sup>16</sup> and Song.<sup>15</sup> Tests were performed with SS 304 and nickel 200 with three gases, that is, argon, helium, and nitrogen. The data covered a wide range of surface characteristics, applied load, thermal and mechanical properties, and gas pressure, which was varied from vacuum to atmospheric pressure. The present model showed good agreement with the data over the entire range of the comparison. The rms relative difference between the model and data was determined to be approximately 7.3%.

## References

- <sup>1</sup>Bejan, A., and Kraus, D., *Heat Transfer Handbook*, Wiley, New York, 2003, Chap. 4.
- <sup>2</sup>Arpaci, V. S., and Larsen, P. S., *Convection Heat Transfer*, Prentice-Hall, Englewood Cliffs, NJ, 1984, Chap. 4.
- <sup>3</sup>Bahrami, M., Yovanovich, M. M., and Culham, J. R., "Thermal Joint Resistances of Nonconforming Rough Surfaces with Gas-Filled Gaps," *Journal of Thermophysics and Heat Transfer*, Vol. 18, No. 3, 2004, pp. 333–339; also AIAA Paper 2004-0822, Jan. 2004.
- <sup>4</sup>Williamson, J. B., Pullen, J., and Hunt, R. T., "The Shape of Solid Surfaces," *Surface Mechanics*, American Society of Mechanical Engineers, New York, 1969, pp. 24–35.
- <sup>5</sup>Greenwood, J. A., and Williamson, B. P., "Contact of Nominally Flat Surfaces," *Proceedings of the Royal Society of London, Series A: Mathematical and Physical Sciences*, Vol. A295, 1966, pp. 300–319.
- <sup>6</sup>Bahrami, M., Culham, J. R., Yovanovich, M. M., and Schneider, G. E., "Review Of Thermal Joint Resistance Models for Non-Conforming Rough Surfaces in a Vacuum," American Society of Mechanical Engineers, ASME Paper HT2003-47051, Fairfield, NJ, July 2003.
- <sup>7</sup>Cooper, M. G., Mikic, B. B., and Yovanovich, M. M., "Thermal Contact Conductance," *International Journal of Heat and Mass Transfer*, Vol. 12, No. 3, 1969, pp. 279–300.
- <sup>8</sup>Carlsaw, H. S., and Jaeger, J. C., *Conduction of Heat in Solids*, 2nd ed., Oxford Univ. Press, London, 1959, Chap. 2.
- <sup>9</sup>Bahrami, M., Culham, J. R., and Yovanovich, M. M., "A Scale Analysis Approach to Thermal Contact Resistance," American Society of Mechanical Engineers, ASME Paper IMECE2003-44097, Fairfield, NJ, July 2003.
- <sup>10</sup>Springer, G. S., "Heat Transfer in Rarefied Gases," *Advances in Heat Transfer*, Vol. 7, 1971, pp. 163–218.
- <sup>11</sup>Kennard, E. H., *Kinetic Theory of Gases*, McGraw-Hill, New York, 1938, Chap. 8.
- <sup>12</sup>Yovanovich, M. M., "Thermal Contact Correlations," *Spacecraft Radiative Transfer and Temperature Control*, edited by T. E. Horton, Progress in Aeronautics and Aerodynamics, Vol. 83, AIAA, New York, 1982, pp. 83–95; also AIAA Paper 81-1164, 1981.
- <sup>13</sup>Song, S., and Yovanovich, M. M., "Correlation of Thermal Accommodation Coefficient for Engineering Surfaces," *National Heat Transfer Conference*, American Society of Mechanical Engineers, Fairfield, NJ, 1987.
- <sup>14</sup>Yovanovich, M. M., DeVaal, J. W., and Hegazy, A. A., "A Statistical Model to Predict Thermal Gap Conductance Between Conforming Rough Surfaces," AIAA Paper 82-0888, June 1982.
- <sup>15</sup>Song, S., "Analytical and Experimental Study of Heat Transfer Through Gas Layers of Contact Interfaces," Ph.D. Dissertation, Dept. of Mechanical Engineering, Univ. of Waterloo, Waterloo, ON, Canada, 1988.
- <sup>16</sup>Hegazy, A. A., "Thermal Joint Conductance of Conforming Rough Surfaces: Effect of Surface Micro-Hardness Variation," Ph.D. Dissertation, Dept. of Mechanical Engineering, Univ. of Waterloo, Waterloo, ON, Canada, 1985.
- <sup>17</sup>Song, S., and Yovanovich, M. M., "Relative Contact Pressure: Dependence on Surface Roughness and Vickers Microhardness," *Journal of Thermophysics and Heat Transfer*, Vol. 2, No. 1, 1988, pp. 43–47.
- <sup>18</sup>Maple7, Waterloo Maple, Release 7, 2001.